

## Multidimensional Scaling of Solid-State Parameters with Plasmon Energy and *In-situ* Spectro-Microscopic Determination and Imaging of Material Properties

V. P. Oleshko

Department of Materials Science & Engineering, University of Virginia, Charlottesville, VA 22904-4745

Measuring material properties is critical to understanding the behavior of contemporary nanostructured materials. However, it is difficult if not sometimes impossible to measure physical (elastic, cohesive, electrical) properties of metastable nanoprecipitates and small particles because they cannot be fabricated in bulk form or because they are too small to be examined by related techniques, such as nanoindentation. Valence electron energy-loss spectroscopy (VEELS) analyzes the spectrum of low-loss excitations (0-50 eV) that involve inter- and intraband transitions and collective excitations of bonding electrons, responsible for many physical properties of solids. Due to the ability to probe electronic structures with high spatial (0.1-1.0 nm) and spectral (0.1-1.5 eV) resolution, VEELS and energy-filtering transmission electron microscopy (EFTEM) are often used to determine phase compositions, dielectric and optical parameters of materials, thus complementing the structural and chemical information accessible in different imaging, diffraction and spectroscopic modes. Furthermore, it was realized [1-3] that it might be possible to determine the elastic moduli, hardness and transport properties of some nanophase materials from their volume plasmon energies,  $E_p = \hbar\omega_p \cong [(\hbar\omega_p^f)^2 + E_g^2]^{1/2}$ , where  $\omega_p^f = [ne^2/(\epsilon_0 m)]^{1/2}$  is the free electron plasma frequency,  $n$  is the valence electron density,  $e$  is the electron charge,  $\epsilon_0$  is the permittivity of vacuum,  $m$  is the electron mass and  $E_g$  is the bandgap energy. As a consequence of the universal binding energy relation (UBER) [4-7], a fundamental scaling relation exists between  $E_p$ , the equilibrium Wigner-Seitz (WS) atomic radius,  $r_{wse}$ , the cohesive energy,  $E_{coh}$ , and the bulk modulus,  $B_m$ , for materials with metallic and covalent bonding:

$$B_m = (1/12\pi)r_{wse}^{-3}E_{coh}\eta^2 = (m_0/4e^2\hbar^2N_{ve})E_{coh}\eta^2(E_p^2 - E_g^2), \quad (1)$$

Here  $r_{wse} = (3/4\pi V_{wse})^{1/3}$ ,  $\eta = r_{wse}/l$  is the dimensionless anharmonicity parameter,  $l$  is the characteristic length describing the width of the binding energy curve or the range over which strong forces act (this sets the range of the Hooke's-law region),  $N_{ve}$  is the number of valence electrons per atom and  $V_{wse}$  is an average volume per atom. From Eqn. (1), elastic, cohesive and electronic properties are not only scaled with  $E_p^2 - E_g^2$  but also interrelated in a multidimensional space. One can employ  $E_p$ -property scaling relations of the type  $P_m = A(E_p^2 - E_g^2)^B$  ( $P_m = B_m, E_{coh}/V_{wse}, n; A$  and  $B$  are *lsf*-parameters for selected materials [6,7]), for *in-situ* VEELS/EFTEM determination and imaging of related properties, as illustrated by examples below. Several forms of carbon (diamond, graphite, diamond-like carbons, hydrogenated and amorphous carbon films) exhibit strong correlations between the energy of the  $\sigma+\pi$ -plasmon peak,  $E_{pmax}$ , ( $E_{pmax} \propto E_p$ ) and the mass density,  $\rho$  (FIG. 1a), and between mechanical hardness,  $H_m$  and  $\rho$  [6-9]. This leads to a 3D-relation between  $E_{pmax}$ ,  $\rho$  and  $H_m$  (FIG. 1b) that can be used to evaluate both the hardness and the density of diesel-engine soot nanoparticles (FIG. 1c). Another example demonstrates plasmon imaging of multiple physical properties (electron density at the boundary of WS cells,  $n_b$ ,  $E_{coh}/V_{wse}$  and  $B_m$ ) of individual metastable  $\gamma$ -TiH<sub>x</sub> nanoprecipitates in an  $\alpha$ -Ti-based alloy (see FIGs. 2b-d, respectively). The property maps were derived from an  $E_p$  map (FIG. 2a) by calculation of corresponding parameters for each pixel from the scaling relations [6,7]. The  $E_p$  map was obtained by correlating the intensity

of each pixel with a particular energy loss in a 20 eV (the volume plasmon in  $\gamma$ -TiH<sub>x</sub>)/18 eV (the volume plasmon in  $\alpha$ -Ti) ratio-image. It displays linear scaled intensities, with precipitates being the brightest and the matrix being darkest and reflect changes in the specimen structure and composition. The technique is denoted as “property-imaging” because its resolution is not compromised relatively to EFTEM. The results indicate that plasmon spectro-microscopic techniques have the potential to determine quantitatively and image multiple solid-state properties at the nanoscale, establishing a new capability for analytical electron microscopy.

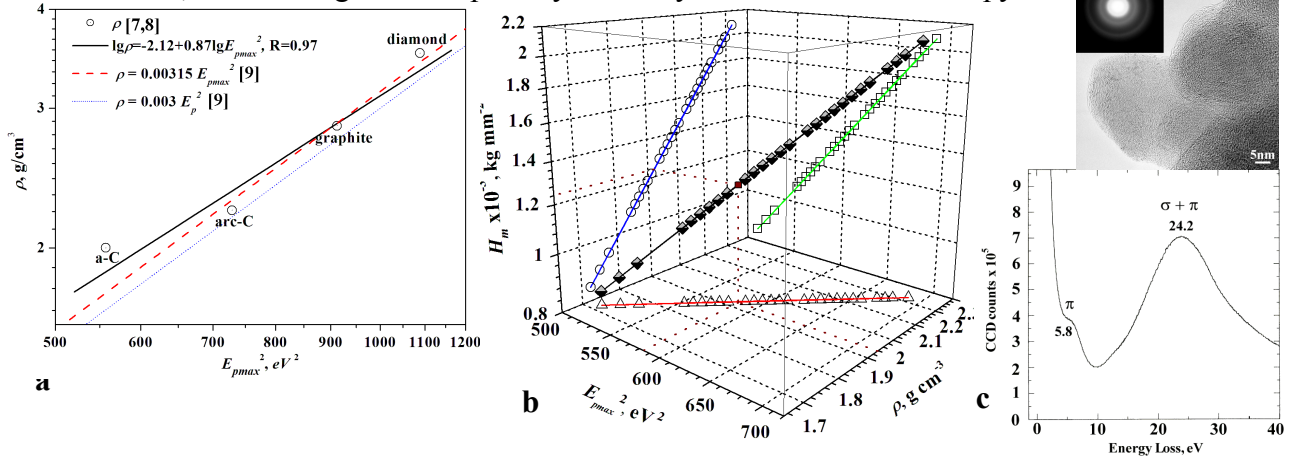


FIG. 1. (a)  $\rho$ - $E_{p(max)}$  correlations for several carbon materials derived from experimental data [7,8] and DFT-FLAPW calculations [9]. (b) 3D- $E_{p(max)}$ - $\rho$ - $H_m$  scaling relation for carbon materials (c) HRTEM, SAED (top inset) and VEEL spectrum of disordered onion-like carbon soot nanoparticles.

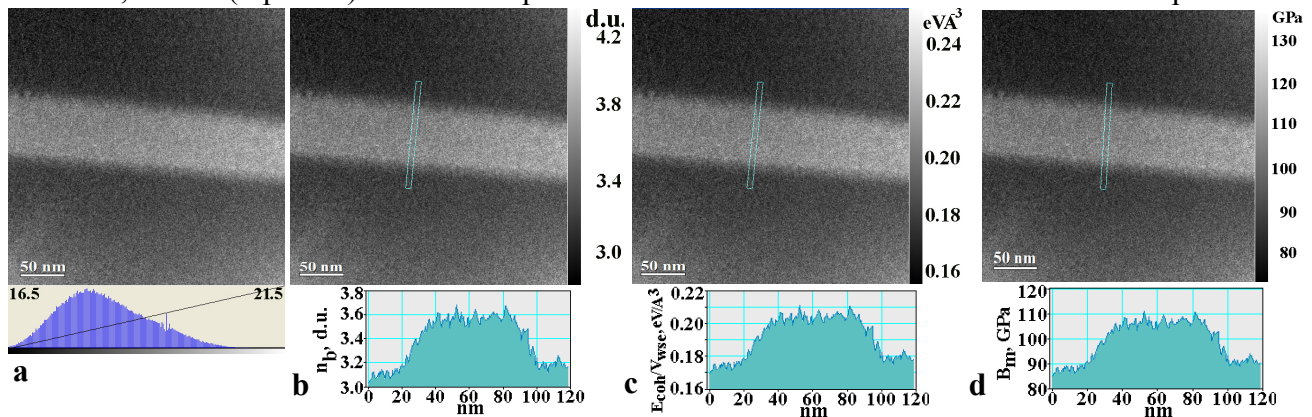


FIG. 2. (a)  $E_p$ -map obtained by rescaling of a 20 eV/18 eV EFTEM ratio-image of a  $\gamma$ -TiH<sub>x</sub> precipitate within the 16.5-21.5 eV range, eV, 3 eV energy window, 0.6 nm x0.6 nm pixel size. (b)  $n_b$  map, d.u. (1d.u.= $6 \times 10^{22}$  electron/cm<sup>3</sup>). (c)  $E_{coh}/V_{wse}$  map, eV/Å<sup>3</sup>. (d)  $B_m$  map, GPa. Rectangular boxes indicate property profiles (bottom insets) taken with a 10-pixel integration window across the precipitate and adjacent  $\alpha$ -Ti matrix.

References

[1] J. J. Gilman, Phil. Mag. 79 (1999) 643. [2] V. P. Oleshko et al., Microsc. Microanal. 8 (2002) 350. [3] L. Laffont et al., Carbon 40 (2002) 767. [4] J. H. Rose et al., Phys. Rev. B 29 (1984) 2963. [5] A. Banerjea, J. R. Smith, Phys. Rev. B 37 (1988) 6632. [6] V. P. Oleshko, J. M. Howe, in: *Mater. Res. Soc. Symp. Proc. Ser.* Vol. 791, Warrendale, PA, 2004, Q9.5.1; *ibid* Vol. 839, 2005, P2.11.1. [7] J.M. Howe, V.P. Oleshko, J. Electron Microsc. 53 (2004) 339. [8] J. Robertson, in: *Diamond and Diamond-Like Films and Coatings, NATO ASI Ser. B.* Vol. 266, N.Y., 1991, 331. [9] J.T. Titantah, D. Lamoen, Phys. Rev. B 70 (2004) 033101-1. [10] This research was supported by the US Department of Energy (Grant No. DE-FG02-01ER45918).